Medicine®

OPEN

Expression of the axon guidance factor Slit2 and its receptor Robo1 in patients with Hirschsprung disease
An observational study

Meng Kong, PhD[a], Tao Zhou, MM[b], Bo Xiang, MD[c],[*]

Abstract

Hirschsprung disease (HD) is a common form of digestive tract malformation in children. However, the pathogenesis of HD is not very clear. This study aimed to investigate the expression of slit guidance ligand 2 (Slit2) and roundabout 1 (Robo1) in patients with HD.

From January 2018 to January 2019, 30 colon specimens from children with HD undergoing surgical resection at the Department of Surgery in Qilu Children's Hospital of Shandong University were obtained. These specimens were divided into the normal segment group, the transitional segment group and the spastic segment group. Immunohistochemical staining, Western blotting, and real-time polymerase chain reaction were used to measure the expression of Slit2 and Robo1 in the intestinal walls of normal, transitional, and spastic segments.

Immunohistochemical staining and Western blot analyses showed high levels of the Slit2 and Robo1 proteins in normal ganglion cells in children with HD, lower levels in transitional ganglion cells, and no expression in spastic segments, with significant differences between groups ($P < .05$). Similarly, the real-time polymerase chain reaction results were consistent with the Western blot analysis results.

The expression of Slit2 and Robo1 decreases significantly in the spastic segment of the intestinal tract in patients with HD.

Abbreviations: ENS = enteric nervous system, HD = Hirschsprung disease, MOD = mean optical density, NGF = nerve growth factor, PVDF = polyvinylidene fluoride, Robo1 = roundabout 1, RT-PCR = real-time polymerase chain reaction, Slit2 = slit guidance ligand 2.

Keywords: enteric nervous system, Hirschsprung disease, immunohistochemistry, roundabout 1, slit guidance ligand 2, Western blot analysis

1. Introduction

Hirschsprung disease (HD), also known as aganglionosis, is one of a common form of developmental malformation of the

[a] Department of Pediatric Surgery, Qilu Children's Hospital of Shandong University, Jinan, China, [b] Department of Pediatric Surgery, Dazhou Central Hospital, Dazhou, China, [c] Department of Pediatric Surgery, West China Hospital of Sichuan University, Chengdu, China.

[*] Correspondence: Bo Xiang, No. 37 Guoxue Alley, Wuhou Distict, Chengdu 610041, China (e-mail: xb_scu_edu@163.com).

digestive tract in children with an incidence of 1/2000 to 1/5000.[1] This disease is mainly characterized by loss of local ganglion cells caused by disorder of neural crest stem cell migration to the intestinal tube, where these cells develop into ganglion cells during embryonic development. It is a typical developmental defect of the enteric nervous system (ENS).[2] At present, the etiology of HD has not been fully elucidated, but most scholars believe that this disease is caused by an interaction between genetic factors and changes in the microenvironment of the intestinal wall.[3] It has been confirmed that changes in the intestinal microenvironment that are related to the occurrence of HD include changes in the extracellular matrix, cell adhesion molecules, nerve growth factor (NGF), neurotrophic factor-3, and tyrosine kinase C.[4]

Slit guidance ligand (Slit) is a protein that has been widely studied and is closely related to neurodevelopment. As one of the main members of the NGF family, Slit has a wide range of biological activities and plays vital roles in the migration, proliferation and differentiation of nerve cells, and the growth of axons.[5] Three Slit family members have been identified: Slit1 to 3 are expressed exclusively in the nervous system. Roundabout (Robo) is a transmembrane protein with 5 Ig-like repeats, 3 fibronectin type III-like repeats in its extracellular region, and 4 short conserved CC0 to 3 motifs in its intracellular region.[6] It can be bound by regulatory proteins that transmit ligand signals in the cytoplasm. The Robo family consists of 4 members, including Robo1 to 3, which are mainly expressed in the nervous system, and Robo4, which is mainly expressed in the vascular

system.[7] The Slit protein binds the extracellular immunoglobu-lin-like domain of its transmembrane receptor Robo through leucine-rich repeat sequences.[8] Ozdinler et al[9] found that Slit2 is the main contributor to the lateral branching of trigeminal axons in the embryonic brainstem. Bagri et al[10] believe that Slit can not only prevent axons from extending to and passing through the midline but also guide axons to specific areas. Whitford et al[11] found that the changes in the cytoskeleton caused by the Slit–Robo interaction alter the growth of growth cones and dendritic arborization through the transfection of dominant-negative Robo and MET-Robo. The aforementioned studies, which specifically examined the central nervous system, confirm that Slit and its receptor Robo are involved in the directional axonal growth, migration and distribution of neurons.

Slit and Robo are involved in regulating cell migration. During the development of the nervous system, immature nerve cells must accurately migrate to the appropriate location before they can differentiate into mature neurons. Studies have found that Slit2 secreted by the choroid plexus and septum of the forebrain in mice inhibits the migration of neuroblasts from the cortical ventricles and the subventricular area and that Slit–Robo signaling prevents the migration of pontine neurons in mice.[12] Slit–Robo signaling causes the formation and maintenance of astrocytic tunnels through interactions with nerve cells and glial cells, thereby facilitating the rapid, directed migration of these neurons in the adult brain. In addition to inhibiting nerve cell migration, members of this family also regulate the migration of nonnerve cells such as muscle cells, white blood cells, tumor cells, and fibroblasts.[13] Slit and Robo also modulate the proliferation and differentiation of nerve cells. Slit1 promotes the elongation of axons of cortical neurons in mice and the peripheral branching of axons of sensory neurons in the trigeminal nerve.[14]

HD is a form of intestinal malformation caused by local ganglion cell loss due to inhibition of the differentiation of neurons migrating into the intestines into ganglion cells. Numerous studies have shown that the Slit2–Robo1 signaling pathway participates in the growth, migration and distribution of axons of neurons in the central nervous system and malignant cancer cells.[15–17] However, details on the expression of Slit2 and Robo1 in the intestines of patients with HD have rarely been reported. Therefore, this study focused on the axon guidance factor Slit2 and assessed the expression and distribution of Slit2 and its receptor Robo1 in diseased segments (spastic and transitional segments) and normal segments of the intestinal tract from children with HD. Determining the expression levels of Slit2 and Robo1 in different parts of the megacolon in children will provide an in-depth and broader understanding of HD.

2. Materials and methods

2.1. Source of specimens

From January 2018 to January 2019, 30 colon specimens were obtained from children with HD undergoing surgical resection at the Department of Surgery of Qilu Children's Hospital of Shandong University. Specimens were taken from 22 males and 8 females aged 3 to 74 months (average age, 14 months). The clinical manifestations of all the children were confirmed to be HD, and the children were confirmed to have common type HD based on barium enema, anorectal manometry, and postopera-tive histopathology. All patients had sporadic disease, denied a

family history of the disease, and received laparoscope-assisted transanal radical resection.

For each colon specimen, 3 segments, that is, a normal segment, a transitional segment and a spastic segment, were divided according to the colon morphology during the operation and the pathological results after the operation. They constituted the normal segment group, the transitional segment group, and the spastic segment group, respectively, with 30 samples in each group. After collection, the samples were immediately stored in a −80°C freezer until Western blotting and real-time polymerase chain reaction (RT-PCR). The remaining specimens were fixed with 4% formaldehyde solution for 12 to 36 hours, routinely dehydrated and then embedded in paraffin for immunohisto-chemical staining.

This study was in accordance with medical ethical standards and was approved by the Ethics Committee of Qilu Children's Hospital of Shandong University (no. ETYY-2017015). Written informed consent was obtained from the guardians of each patient.

2.2. Hematoxylin-eosin staining

Consecutive sections of the paraffin-embedded sample were generated at a thickness of approximately 4 mm. HE staining was performed. The structure of the intestinal tissue was observed under an optical electron miscroscope (Leica, Germany). For each section, 5 high-power fields (×400) were randomly selected. The development of ganglion cells in the intestinal tract was assessed based on the average number and diameter of the cells within the myenteric plexus.

2.3. Immunohistochemistry

Paraffin sections from the normal segment group, transitional segment group, and spastic segment group were selected for immunohistochemical analysis, placed in an oven at 60°C for 2 hours, and then stored at room temperature. Next, the sections were dewaxed in xylene and water and incubated with 3% hydrogen peroxide (H_2O_2) at room temperature for 15 to 30 minutes. After treatment with the citrate antigen retrieval solution (pH 6.0), the tissues were cooled to room temperature, and incubated with mouse antihuman primary antibodies against Slit2 and Robo1 (1:200) (Beijing Bioss Co., Ltd.) overnight in a refrigerator at 4°C. The next day, after washing with phosphate-buffered saline, the tissues were incubated with a goat antimouse secondary antibody at room temperature for approximately 20 minutes. After development with diaminobenzidine, the tissues were stained with hematoxylin, dehydrated, cleared, and sealed. A total of 5 high-power fields (400×) were randomly selected from each section, and the staining intensity of 5 positive cells in each field was determined, and the percentage of positive cells was calculated. Yellow-stained cells were considered positive cells, while those without staining were considered negative cells. The percentage of positive cells was scored as follows[18,19]: ≤10%; 11% to 50%; 51% to 75%; and ≥75%. In addition, the staining intensity was scored as follows: 0, unstained; 1, light yellow; 2, pale brown; and 3, tan. The total score was obtained by multiplying the percentage of positive cells score and the staining intensity score and was used to assess staining as follows: 0, negative (−); 1 to 3, weakly positive (+); 4 to 6, positive (++); and >7, strongly positive (+++). All tissue sections were observed under a light microscope (Leica, Germany) (400×). Images were

acquired and imported into Leica Qwin image analysis software (Forma Scientific, Germany), and 5 visual fields were randomly selected from each section. Slit2 and Robo1 protein expression were analyzed using Image-ProPlus 6.0 image analysis software (Forma Scientific, Germany). The mean optical density (MOD) was calculated, and the average MOD in 5 visual fields was calculated as a measure of the expression in each sample.

2.4. Western blot analysis

Full-thickness tissue specimens from normal, transitional, and spastic segments of the intestine were selected. Total protein was extracted using a whole protein extraction kit (Beyotime Institute of Biotechnology, China). The protein content was determined by the bicinchoninic acid disodium method (Beyotime Institute of Biotechnology, China). The specimens were cryopreserved at −20°C for subsequent detection. Sample buffer was added to 60 μL total protein, and the samples were boiled for 5 minutes. After 10% sodium dodecyl sulfate-polyacrylamide gel electrophoresis, the proteins were transferred onto a polyvinylidene fluoride (PVDF) membrane. After blocking with a solution containing 5% skim milk powder, the PVDF membranes were incubated with Slit2 and Robo1 antibodies (1:500) (Abcam, ab134166 and ab256791) or a β-actin antibody (1:1000) (Beijing Bioss Co., bs-0293R) and then washed twice. Then, an alkaline phosphatase-labeled goat anti-rabbit IgG secondary antibody (working concentration, 1:10,000) (Shanghai Long Island Antibody Diagnostica, 0295G) was added for hybridization for 1 hour at room temperature. PVDF membranes were placed directly in a dual-band infrared imaging system (LI-COR Biosciences), scanned, and analyzed. The density of each amplified band was analyzed, and protein expression was calculated using the relative gray value: relative gray value = (gray value of the target protein band/gray value of the internal reference band).

2.5. Real-time polymerase chain reaction

The Slit2 and Robo1 genes were amplified using PCR. The primers were designed by referring to the MEDLINE database of the US National Library of Medicine and synthesized with the assistance of Dalian Takara Co., Ltd. (Table 1). Total RNA was extracted using Trizol reagent. The main reagents included chloroform (Sinopharm Chemical Reagent Co., Ltd., China; 75-62-7), isopropanol (Sinopharm Chemical Reagent Co., Ltd.; 67-63-0), 75% ethanol (Sinopharm Chemical Reagent Co., Ltd.; 64-17-5), RNase-free water (Solarbio, Beijing, China; r1600), and Trizol RNA extraction reagent (Thermo Fisher Scientific, Massachusetts, MA, USA; bv15596026). Full-thickness tissue specimens of normal, transitional, and spastic segments of the

intestine were selected for total RNA extraction. The concentration of RNA was determined using ultraviolet spectrophotometry (Biometra). The extracted RNA was stored at −80°C. Three microliters of RNA were used for reverse transcription. Complementary DNA was synthesized by reverse transcription using a reverse transcription kit (Dalian Takara Co., Ltd.). PCR was performed using a SYBR Premix Ex TaqTM quantitative fluorescence kit (Dalian Takara Co., Ltd.). The complementary DNA samples were collected and diluted 10 times to determine the efficiency of qPCR amplification. Additionally, a reaction tube without template was used as a negative control. The Ct values of β-actin and the target gene in each sample were calculated. To reduce error, each sample was analyzed twice. The experiment was repeated thrice, and averages were obtained. The main instrument was a real-time fluorescence PCR instrument (QS5; ABI). The relative expression of the gene in the sample was calculated, and the following data were calculated according to the Ct value: $\Delta Ct = Ct_{targetgene} - Ct_{referencefactor}$; $\Delta\Delta Ct = \Delta Ct_{targetgene} - \Delta Ct_{referencefactor}$; and the expression of the target gene $= 2^{-\Delta\Delta Ct}$.

2.6. Statistical analysis

All the data were analyzed using SPSS 22.0 (SPSS, Inc., Chicago, IL). Measurement data with a normal distribution are expressed as the mean ± standard deviation (x ± s). A t test was used to compare data between 2 groups, and ANOVA followed by Bonferroni correction was used to compare data among multiple groups. $P = .05$ was used as the cutoff, with $P < .05$ being considered statistically significant.

3. Results

3.1. HE staining and observations

In the normal segments, normal nerve plexuses were observed in the intramuscular and submucosal areas of the intestinal wall, which were densely distributed along the intestinal tract. Ganglion cells with a normal shape and number were observed within the nerve plexus. These cells were well developed. They had a large cytoplasm with a centrally located round nucleus and obvious nucleolus, and displayed normal development in all layers of the intestinal wall (Fig. 1A). In the transitional segments, proliferative nerve plexuses were observed in the intramuscular and submucosal areas of the intestinal wall. The ganglion cells in the nerve plexus were poorly developed, and they were smaller than normal cells. The nucleolus was less noticeable and the cytoplasmic volume was reduced. The number of the nerve plexuses was less than that in the normal group. The smooth muscle presented a locally disordered arrangement (Fig. 1B). In

Table 1

Primer sequences and amplified fragment lengths of GAPDH, Slit2, and Robo1.

| Gene	Primer sequence	Annealing temperature (°C)	Amplified fragment length (bp)
GAPDH	Upstream: 5′-GCACCGTCAAGGCTGAGAAC-3′ Downstream: 5′-TGGTGAAGACGCCAGTGGA-3′	63	138
Slit2	Upstream: 5′-CCTGCCAGCACGATTCAAAG-3′ Downstream: 5′-ATCAGTTCCTCCTTGGTTTCGTAG-3′	64	91
Robo1	Upstream: 5′-TGTTGCTTTGGGACGGACTGTA-3′ Downstream: 5′-AAATCGGCTGGATGACTGTGG-3′	64	133

Robo1 = roundabout 1, Slit2 = slit guidance ligand 2.
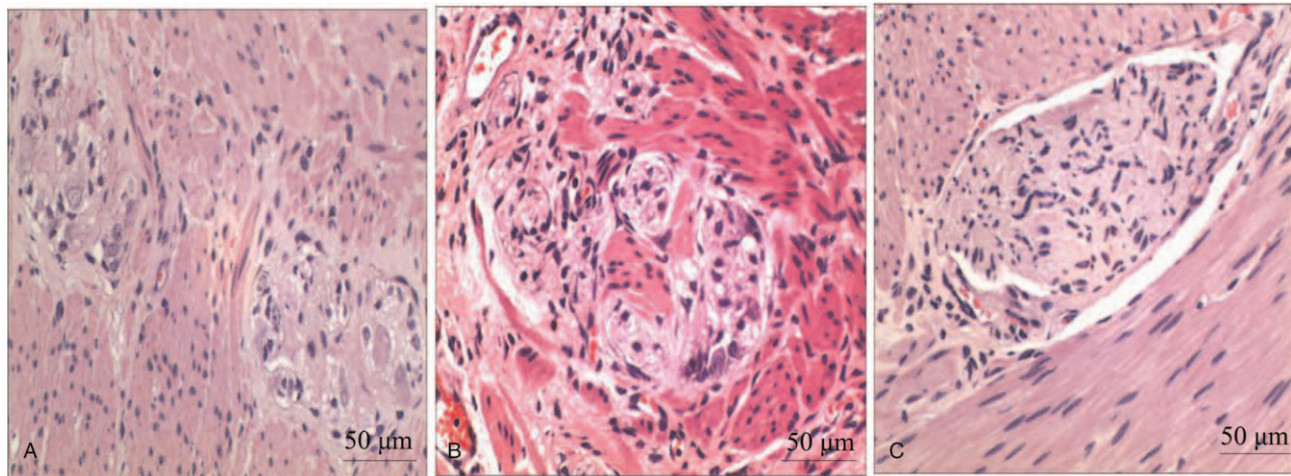
Figure 1. Hematoxylin-eosin staining showing the outcomes of the 3 groups (×400). (A) The normal segment group. The number of ganglion cells was normal, and the cells were well developed with a large volume of cytoplasm. The nucleus was centrally located, with a noticeable nucleolus. (B) The transitional group. The ganglion cells were poorly developed. The cells had a smaller morphology, a less noticeable nucleolus, and less cytoplasm than the normal cells. (C) The spastic segment group. No ganglion cells were observed, and a small portion of the nerve plexuses presented hyperplasia.

the spastic segment group, no nerve plexuses were observed in the intramuscular and submucosal areas. The diameter of the nerve plexuses was smaller, and a small portion presented with hyperplasia; the myometrial cells were also disordered (Fig. 1C). The normal segment groups showed a significant difference in the diameter of the nerve plexus compared with the transitional group and the spastic group ($P < .05$), whereas no significant difference was observed between the latter 2 groups ($P > .05$). The normal segment group also showed significant differences in the diameter and number of ganglion cells compared with the transitional group ($P < .05$) (Table 2).

3.2. Immunohistochemical staining for slit guidance ligand 2 in Hirschsprung disease tissues

Immunohistochemical staining was performed to assess the expression and distribution of the Slit2 protein in the intestines of children with HD, and Slit2 was expressed at high levels in intestinal plexus cells, as indicated by strong staining, while a dark brown mass in the cytoplasm, significant Slit2 expression and no obvious nuclear staining were observed in ganglion cells from the normal segment group (Fig. 2A). In addition, Slit2 was expressed at a low level in ganglion cells in the transitional segment group, as indicated by positive staining. Pale yellow flaky particles were seen in the cytoplasm of ganglion cells, and no obvious staining was observed in the nucleus (Fig. 2B). However, no obvious ganglion cells or Slit2 expression was observed in the spastic segment group, as indicated by negative staining (Fig. 2C). Immunohistochemical staining showed a gradual decrease in the

expression of Slit2 in the normal, transitional and spastic segment groups. According to the statistical analysis of MOD values, the expression level of Slit2 in the normal segment group was significantly higher than that in the transitional segment group (126.73 ± 9.77 vs 89.67 ± 14.82; $P < .05$), specifically, the level of Slit2 in the normal segment group was 1.41 times higher than that in the transitional segment group. Thus, the Slit2 expression level gradually increased in the normal segment group but decreased in the transitional segment group. There were ganglion cells in the transitional segment group, but there were fewer ganglion cells in this group than in the normal segment group. Similarly, a significantly higher Slit2 content was observed in the transitional segment group than in the spastic segment group (89.67 ± 14.82 vs 53.77 ± 14.40); specifically, the Slit2 content in the transition group was 1.67 times higher than that in the spastic segment group ($P < .05$). The most obvious difference was the 2.36 times higher Slit2 level in the normal segment group than that in the spastic segment group, and this difference was significant ($P < .05$). The highest expression of Slit2 was observed in the normal segment group, and the lowest expression was detected in the spastic segment group (Table 3).

3.3. Immunohistochemical staining for roundabout 1 in Hirschsprung disease tissues

Similarly, immunohistochemical staining was conducted to assess the expression and distribution of the Robo1 protein in the intestinal tracts of children with HD. Robo1 was mainly expressed in the intestinal plexus cells of the normal segment

Table 2

The diameters of the nerve plex us and the numbers and diameters of the ganglion cells in each group ($\bar{x} \pm s$).

Group	Number	Diameter of the nerve plexus (μm)	Diameter of ganglion cells (μm)	Number of ganglion cells
Normal	30	60.13 ± 10.25	18.32 ± 1.34	6.39 ± 1.84
Transitional	30	$38.29 \pm 5.86^{*}$	$13.81 \pm 0.97^{*}$	$3.55 \pm 1.18^{*}$
Spastic	30	$36.64 \pm 4.92^{*}$	–	–

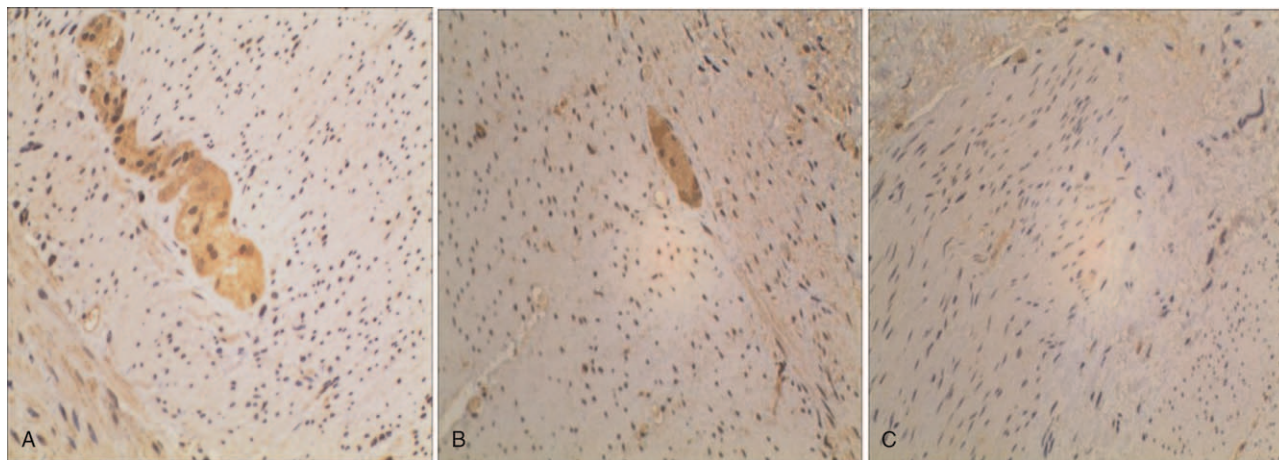$^{*} P < .05$, transitional and spastic groups vs the normal group.

Figure 2. Expression of Slit2 in different segments of the intestines of children with HD (immunohistochemical staining, 400× magnification). (A) Slit2 was expressed in a large number of nerve clusters in the normal group, as indicated by dark brown staining. (B) Slit2 was expressed at a low level in the transitional segment group, as indicated by light yellow staining. (C) Slit2 was not expressed in the spastic segment group. The arrow in the figure shows the localization of the Slit2 protein. HD = Hirschsprung disease, Slit2 = slit guidance ligand 2.

<div class="table">

Table 3

Comparison of the MOD values of Slit2 and Robo1 in each intestinal segment in the 3 groups (mean ± SD).

Group	Number of patients (n)	Slit2	Robo1
Normal segment	30	126.73 ± 9.77	119.67 ± 12.93
Transitional segment	30	$89.67 \pm 14.82^{*}$	$93.87 \pm 15.87^{*}$
Spastic segment	30	$53.77 \pm 14.40^{*\dagger}$	$42.93 \pm 14.03^{*\dagger}$
P		$<.05$	$<.05$

MOD = mean optical density, Robo1 = roundabout 1, Slit2 = slit guidance ligand 2.
The transitional segment group and the spastic segment group were compared with the normal segment group.
$^{*}P < .05$. The spastic segment group was compared with the transitional segment group.
$^{\dagger}P < .05$.

</div>

group, as indicated by strong staining. The nuclei and cytoplasm of ganglion cells were stained dark brown, and the expression level in the cytoplasm was higher than that in the nuclei (Fig. 3A). In addition, Robo1 was expressed in ganglion cells in the transitional segment group, but was expressed at lower levels in ganglion cells in this group than in the normal segment group; additionally, pale yellow granules were observed in the nuclei and cytoplasm of ganglion cells (Fig. 3B). However, no obvious ganglion cells and no Robo1 expression were detected in the spastic segment group (Fig. 3C). According to the immunohistochemical staining, Robo1 expression decreased gradually in the normal segment group, the transitional segment group, and the spastic segment group, with the highest expression observed in the normal segment group and the lowest expression observed in
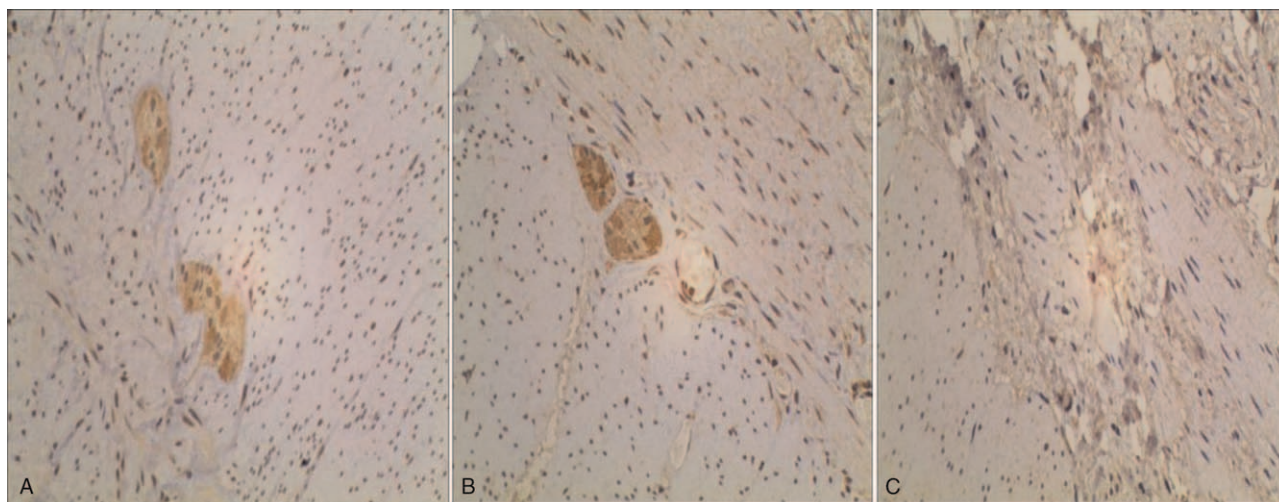

Figure 3. Expression of Robo1 in different segments of the intestines of children with HD (immunohistochemical staining, 400× magnification). (A) Robo1 was abundantly expressed in normal nerve clusters, as indicated by dark brown staining. (B) Robo1 was expressed at a low level in the transitional group, as indicated by light yellow staining. (C) Robo1 was not expressed in the spastic segment group. The localization of the Robo1 protein is shown by the red arrow in the figure. HD = Hirschsprung disease, Robo1 = Roundabout 1.

the spastic segment group. According to statistical analysis of MOD values, the content of Robo1 in the normal segment group was significantly higher than that in the transitional segment group (119.67 ± 12.93 vs 93.87 ± 15.87); specifically, the content of Robo1 in the normal segment group was 1.27 times higher than that in the transitional segment group ($P < .05$). Similarly, the content of Robo1 in the transitional segment group was significantly higher than that in the spastic segment group (93.87 ± 15.87 vs 42.93 ± 14.03); specifically, the content of Robo1 in the transitional segment group was 1.67 times higher than that in the spastic segment group ($P < .05$). Most obviously, the Robo1 content in the normal segment group was 2.19 times higher than that in the spastic segment group, and this difference was significant ($P < .05$) (Table 3).

3.4. Western blot analysis of slit guidance ligand 2 and roundabout 1 levels in Hirschsprung disease tissues

Western blotting was used to measure the levels of the Slit2 and Robo1 proteins in the intestines of children with HD. The Slit2 and Robo1 proteins were expressed in the normal, transitional, and spastic segments, and the expression levels gradually decreased. The expression level was highest in the normal segment group and lowest in the spastic segment group (Fig. 4A). Statistical analyses of the protein expression data showed significantly higher levels of Slit2 and Robo1 in the normal segment group than in the transitional segment group (0.70 ± 0.12 vs 0.54 ± 0.09 and 0.63 ± 0.08 vs 0.39 ± 0.08, respectively) ($P < .05$). Similarly, the contents of Slit2 and Robo1 in the

transitional segment group were significantly higher than those in the spastic segment group (0.54 ± 0.09 vs 0.35 ± 0.08 and 0.39 ± 0.08 vs 0.22 ± 0.07, respectively) ($P < .05$). The most obvious difference was the significantly higher levels of Slit2 and Robo1 in the normal segment group than in the spastic segment group (0.70 ± 0.12 vs 0.35 ± 0.08 and 0.63 ± 0.08 vs 0.22 ± 0.07, respectively) (Fig. 4B).

3.5. Analysis of slit guidance ligand 2 and roundabout 1 mRNA expression in Hirschsprung disease tissues

We measured the expression levels of the Slit2 and Robo1 mRNAs in HD tissues using RT-PCR. The Slit2 mRNA and Robo1 mRNA were expressed in the normal, transitional and spastic segments, and the expression levels gradually decreased. The results of the RT-PCR analysis of mRNA expression were consistent with the results of Western blot analysis of protein expression. The expression levels of Slit2 and Robo1 in the normal segment group were 1.21 times and 1.26 times higher, respectively, than those in the transitional group, and the differences were statistically significant ($P < .05$). The expression levels of Slit2 and Robo1 in the transitional segment group were 1.32 times and 1.38 times higher, respectively, than those in the spastic segment group, and the differences were significant ($P < .05$). The most obvious differences in expression were between the normal segment and spastic segment groups; the expression levels of Slit2 and Robo1 in the normal segment group were 1.60 times and 1.73 times higher, respectively, than those in the spastic segment group, and the differences were significant ($P < .05$) (Fig. 5 and Table 4).

4. Discussion

This study is innovative because it is the first to report that Slit2 and its receptor Robo1 are expressed in the intestines of children with HD. In this report, we assessed the expression of Slit2 and Robo1 in HD tissues.

In a recent study, Zhao and Mommersteeg[20] found that Slit2 and Robo1 are expressed at very high levels in the hearts of drosophilid flies, zebrafish, and mice, suggesting that they may participate in the regeneration and migration of cardiac cells and chamber formation. Some studies performed abroad have also found that Slit2 and Robo1 are expressed in thyroid and cervical cancer specimens,[21,22] indicating that they may be related to
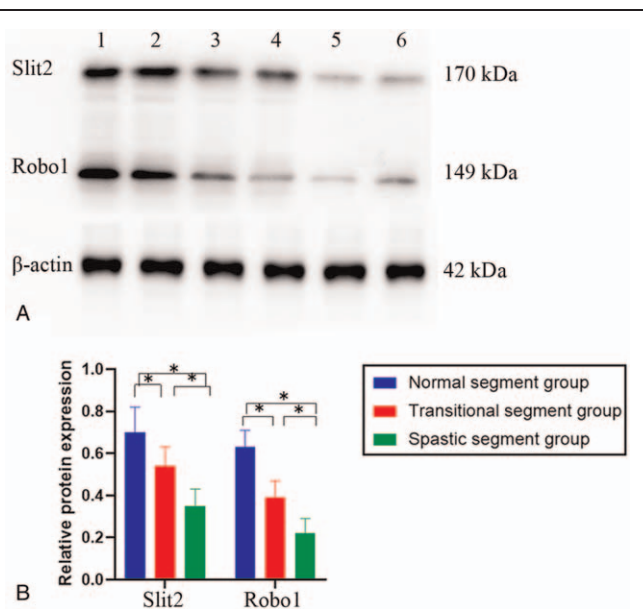

Figure 4. Slit2 and Robo1 protein expression in the 3 groups (30 tissues per group). (A) Electrophoretograms showing Slit2 and Robo1 protein expression in the 3 groups. The highest levels of the Slit2 and Robo1 proteins were observed in the normal segment group, the lowest expression levels of Slit2 and Robo1 were detected in the spastic segment group, and the expression levels of Slit2 and Robo1 in the transitional segment group were between those in the normal segment group and those in the spastic segment group. (B) Histogram of protein expression in the different groups. The pairwise comparison revealed that the difference was significant; *$P < .05$. 1 and 2, the normal segment group; 3 and 4, the transitional segment group; 5 and 6, the spastic group. Robo1 = roundabout 1, Slit2 = slit guidance ligand 2.
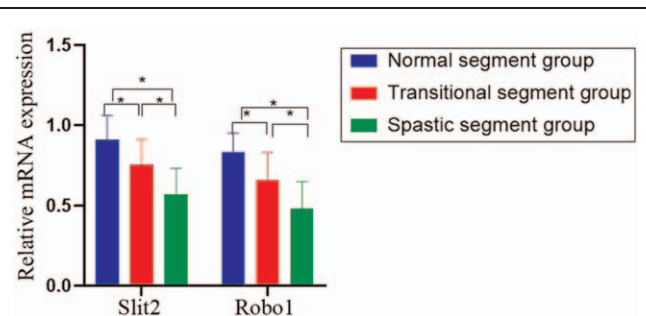

Figure 5. Expression levels of the Slit2 and Robo1 mRNAs in different intestinal segments. The highest expression levels of Slit2 and Robo1 were detected in the normal segment group and the lowest levels were observed in the spastic segment group. Pairwise comparison revealed that the difference was significant; *$P < .05$. Robo1 = roundabout 1, Slit2 = slit guidance ligand 2.

Table 4

Comparison of Slit2 and Robo1 mRNA expression in each intestinal segment among the 3 groups (means ± SD).

Group	Number of patients (n)	Slit2	Robo1
Normal segment	30	0.91 ± 0.15	0.83 ± 0.12
Transitional segment	30	0.75 ± 0.16*	0.66 ± 0.17*
Spastic segment	30	0.57 ± 0.16*†	0.48 ± 0.17*†
P		<.05	<.05

Robo1 = roundabout 1, Slit2 = slit guidance ligand 2.

The transitional segment group and the spastic segment group were compared with the normal segment group.

* $P < .05$. The spastic segment group was compared with the transitional segment group.

† $P < .05$.

tumor growth and metastasis. These results are consistent with our findings that Slit2 and Robo1 are not only present in the central nervous system but also expressed in the ENS, cardiovascular system and tumor tissues. They may play an important role in the regeneration, migration, and orientation of neurons. Axon guidance is a basic process in the development of neurons.[23] In the central nervous system of vertebrates, the axons of neurons must grow properly to reach their target sites and exert their effects. The nerve growth guidance factors that have been identified thus far include members of the Ephrin family, Netrin family, Semaphorin family, and Slit family.[24] Slit2 and its receptor Robo1 may exert their effects through the Slit2–Robo1 signaling pathway. After the Slit protein binds to the extracellular immunoglobulin-like domain of its transmembrane receptor Robo through leucine-rich repeats, Slit–Robo GTPase activating protein molecules, which are coupled with the Robo intracellular domain in cells, are activated. These molecules regulate the polarity-dependent distribution of cytoskeleton-associated proteins and actins in cells and guide the migration of nerve cells and the growth of axons to produce biological effects.[8,25] Therefore, abnormal expression of Slit or Robo blocks signal transduction by nerve cells, thereby leading to the occurrence of diseases.

In addition, Slit2 and its receptor Robo1 were expressed in the intestines of children with HD and in transitional segments of HD tissues, but Slit2 and Robo1 expression in these segments were slightly weaker than the levels observed in normal segments. However, the levels of the Slit2 and Robo1 proteins were significantly decreased or were almost absent in spastic segments. Similarly, the expression levels of the Slit2 and Robo1 mRNAs were significantly lower in the spastic segments than in the transitional and normal segments of children with HD. Moreover, the expression levels of the Slit2 and Robo1 mRNAs in transitional segments were significantly lower than those in normal segments ($P < .05$). Based on these results, Slit2 and Robo1 expression were downregulated in the diseased intestines of children with HD. Kaur et al[26] found significantly decreased expression levels of Slit2 and Robo1 in the brains of rats subjected to hypoxia-ischemia, suggesting that Slit2 may contribute to the attenuation of neuronal apoptosis. Li et al[27] observed a significant decrease in Robo1 expression after spinal cord injury in vertebrates, which suggests that the Robo1 signaling pathway may promote axonal regeneration and synaptic formation in neurons, providing a novel strategy for the treatment of spinal cord injury. In our previous experiment,[28] it was found that the expression of glial cell-derived neurotrophic factor was downregulated in children with congenital anorectal malformation and the terminal rectum in

animal models. This decrease in glial cell-derived neurotrophic factor expression might affect the development and maturation of the ENS. These results indicate that NGFs such as Slit2 and Robo1 are abnormally expressed in the nervous system. Interestingly, these results are basically consistent with our findings. Decreased expression of Slit2 and Robo1 affects normal Slit–Robo signal transduction, further affecting the proliferation, differentiation, migration, and maturation of ganglion cells. Moreover, we assessed the expression of the Slit2 and Robo1 proteins in different intestinal segments of HD tissues and found that the distribution pattern of these molecules was consistent with that in ganglion cells in children with HD. This finding also suggests that Slit2 and Robo1 may participate in the development and function of the ENS by interacting with each other during the development of ganglion cells, thereby leading to dyskinesia of diseased intestinal segments and changes in intestinal morphology. This finding provides a new direction for elucidating the pathogenesis of HD.

We studied the colons of children with HD by collecting normal segments, transitional segments, and spastic segments. The expression of Slit2 and Robo1 in different colon segments of patients with HD was measured, and we observed significantly higher expression of these molecules in normal segments than in spastic and transitional segments. Additionally, the expression levels of both of these molecules were consistent with the number of ganglion cells in the gut; a higher number of ganglion cells was associated with higher Slit2 and Robo1 expression, and a lower number of ganglion cells was associated with lower expression of these molecules. Tang et al[29] documented significantly lower levels of Slit2 in the colons of normal children than in the intestines of children with HD, and Slit2 inhibited cell migration, while knockout of Robo1 reversed this inhibition, suggesting that the Slit2/Robo1 pathway is also involved in the pathogenesis of HD. Interestingly, our findings were inconsistent with those reported by Tang et al.[29] We propose that this difference may be attributed to the division of the patients in the study by Tang et al into 2 groups, and the children in the normal group suffered from different diseases, which may have led to erroneous findings for Slit2 expression in children with normal colons. The increased expression of Slit2 in the intestines of HD patients may be due to negative feedback regulation in the body. As Slit2 is a protective factor, when lesions occur in the intestine, Slit2 may migrate to the intestine, thereby playing roles in nerve growth and migration. The expression of Slit2 in the HD group was higher than that in the normal group. Therefore, we speculated that Slit2 and Robo1 may promote the migration of intestinal nerve cells and that intestinal ganglia cells may also secrete Slit2 and Robo1 proteins, which exert mutual effects on promotion, coordination and neuronal guidance. This conclusion is consistent with our previous hypothesis, but the protective effects of Slit2 and Robo1 are not sufficient to resist the occurrence of HD.

There are some limitations to this study. First, this study preliminarily investigated the expression of Slit2 and Robo1 in children with HD and did not elucidate the roles of these molecules in the development of HD. Cell migration experiments and animal experiments must be conducted to clarify the roles of Slit2 and Robo1 in the development of HD. Second, the results of this study did not reveal the stage of HD at which the expression of Slit2 and Robo1 becomes abnormal. This question remains to be answered in the future.

In conclusion, abnormal expression of Slit2 and its receptor Robo1 was observed in the diseased intestines of children with

HD. The results of this study may broaden and deepen our understanding of HD.

Author contributions

Conceptualization: Meng Kong.
Data curation: Tao Zhou.
Formal analysis: Meng Kong.
Funding acquisition: Bo Xiang.
Investigation: Meng Kong, Tao Zhou.
Methodology: Bo Xiang.
Project administration: Bo Xiang.
Resources: Bo Xiang.
Validation: Tao Zhou.
Visualization: Tao Zhou.
Writing – original draft: Meng Kong.
Writing – review & editing: Bo Xiang.

References

[1] Ambartsumyan L, Smith C, Kapur RP. Diagnosis of Hirschsprung disease. Pediatr Dev Pathol 2020;23:8–22.
[2] Shimojima N, Kobayashi M, Kamba S, et al. Visualization of the human enteric nervous system by confocal laser endomicroscopy in Hirschsprung's disease: an alternative to intraoperative histopathological diagnosis? Neurogastroenterol Motil 2020;32:e13805.
[3] Lantieri F, Gimelli S, Viaggi C, et al. Copy number variations in candidate genomic regions confirm genetic heterogeneity and parental bias in Hirschsprung disease. Orphanet J Rare Dis 2019;14:270.
[4] Rocco ML, Soligo M, Manni L, Aloe L. Nerve growth factor: early studies and recent clinical trials. Curr Neuropharmacol 2018;16:1455–65.
[5] Kim M, Lee CH, Barnum SJ, Watson RC, Li J, Mastick GS. Slit/Robo signals prevent spinal motor neuron emigration by organizing the spinal cord basement membrane. Dev Biol 2019;455:449–57.
[6] Bisiak F, McCarthy AA. Structure and function of roundabout receptors. Subcell Biochem 2019;93:291–319.
[7] Dai C, Gong Q, Cheng Y, Su G. Regulatory mechanisms of Robo4 and their effects on angiogenesis. Biosci Rep 2019;39:5–13.
[8] Tong M, Jun T, Nie Y, Hao J, Fan D. The role of the Slit/Robo signaling pathway. J Cancer 2019;10:2694–705.
[9] Ozdinler PH. Expanded access: opening doors to personalized medicine for rare disease patients and patients with neurodegenerative diseases. FEBS J 2020;288:1457–61.
[10] Bagri P, Anipindi VC, Nguyen PV, Vitali D, Stämpfli MR, Kaushi C. Novel role for Interleukin-17 in enhancing type 1 helper T cell immunity in the female genital tract following mucosal herpes simplex virus 2 vaccination. J Virol 2017;91:e01234–317.
[11] Whitford B, Nadel AL, Fish JD. Burnout in pediatric hematology/oncology-time to address the elephant by name. Pediatr Blood Cancer 2018;65:e27244.
[12] Taroc EZM, Lin JM, Tulloch AJ, Jaworski A, Forni PE. GnRH-1 neural migration from the nose to the brain is independent from Slit2, Robo3 and Nell2 signaling. Front Cell Neurosci 2019;13:70.
[13] Caipo L, González-Ramírez MC, Guzmán-Palma P, et al. Slit neuronal secretion coordinates optic lobe morphogenesis in drosophila. Dev Biol 2020;458:32–42.
[14] Rafipay A, Dun XP, Parkinson DB, Erskine L, Vargesson N. Knockdown of slit signaling during limb development leads to a reduction in humerus length. Dev Dyn 2020;21:
[15] Fan X, Yang H, Kumar S, et al. SLIT2/ROBO2 signaling pathway inhibits nonmuscle myosin IIA activity and destabilizes kidney podocyte adhesion. JCI Insight 2016;1:e86934.
[16] Ong HS, Tey KY, Ke M, et al. A pilot study investigating anterior segment optical coherence tomography angiography as a non-invasive tool in evaluating corneal vascularisation. Sci Rep 2021;11:1212.
[17] Rezniczek GA, Grunwald C, Hilal Z, et al. ROBO1 expression in metastasizing breast and ovarian cancer: SLIT2-induced chemotaxis requires heparan sulfates (heparin). Anticancer Res 2019;39:1267–73.
[18] Khoury JD, Wang WL, Prieto VG, et al. Validation of Immunohistochemical assays for integral biomarkers in the NCI-MATCH EAY131 clinical trial. Clin Cancer Res 2018;24:521–31.
[19] Mohammadi Z, Hayati Roodbari N, Parivar K, Salehnia M. Supplementation of culture media with lysophosphatidic acid improves the follicular development of human ovarian tissue after xenotransplantaion into the back muscle of γ-irradiated mice. Cell Journal 2020;22:358–66.
[20] Zhao J, Mommersteeg MTM. Slit-Robo signalling in heart development. Cardiovasc Res 2018;114:794–804.
[21] Jeon MJ, Lim S, You MH, et al. The role of SLIT2 as a tumor suppressor in thyroid cancer. Mol Cell Endocrinol 2019;483:87–96.
[22] Shi RL, Qu N, Liao T, et al. Expression clinical significance and mechanism of SLIT2 in papillary thyroid cancer. Int J Oncol 2016;48:2055–62.
[23] Gokoffski KK, Jia X, Shvarts D, Xia G, Zhao M. Physiologic electrical fields direct retinal ganglion cell axon growth in vitro. Invest Ophthalmol Vis Sci 2019;60:3659–68.
[24] Seiradake E, Jones EY, Klein R. Structural perspectives on axon guidance. Annu Rev Cell Dev Biol 2016;32:577–608.
[25] Pérez C, Sawmiller D, Tan J. The role of heparan sulfate deficiency in autistic phenotype: potential involvement of Slit/Robo/srGAPs-mediated dendritic spine formation. Neural Dev 2016;18:11.
[26] Kaur H, Xu N, Doycheva DM, Malaguit J, Tang J, Zhang JH. Recombinant SLIT2 attenuates neuronal apoptosis via the ROBO1-srGAP1 pathway in a rat model of neonatal HIE. Neuropharmacology 2019;158:107727.
[27] Li Y, Gao Y, Xu X, et al. SLIT2/ROBO1 promotes synaptogenesis and functional recovery of spinal cord injury. Neuroreport 2017;28:75–81.
[28] Kong M, Wu Y, Liu Y. The impact of HuD protein on the intestinal nervous system in the terminal rectum of animal models of congenital anorectal malformation. Mol Med Rep 2017;16:4797–802.
[29] Tang W, Tang J, He J, et al. SLIT2/ROBO1-miR-218-1-RET/PLAG1: a new disease pathway involved in Hirschsprung's disease. J Cell Mol Med 2015;19:1197–207.